Supplementary Materials

A computerized morphometric approach was used to batch process 699 liver images, reducing bias and decreasing image processing time. Specifically, we sought to quantify "putative" lipid content in the form of vacuoles in digitally imaged, H&E stained liver sections from each treatment group and their controls. Such a method has been shown to correlate with both visual estimations and biochemical determinations of micro- and macrovesicular steatosis in humans and rats (Li *et al.*, 2011; Liquori *et al.*, 2009). However, the software packages used for such analyses can be expensive. ImageJ (Rasband, 2014) is a free and open source software reliably used in multiple scientific fields for image quantification (Collins, 2007).

The unequivocal identification of lipids presented a challenge because fat-specific stains were not used, and we saw a large degree of heterogeneity among our images (regarding vacuolation and other features). Our simple, custom Java macro (see below) was used to quantify the amount of lipid in every image regardless of vacuole distribution and staining variation. Because we wanted to employ batch processing, this macro employed various assumptions. ImageJ was set to measure all sizes (0 to infinity) and circularities (0-1.00) to capture small vacuoles (*e.g.*, microvesicular vacuolation) as well as large and/or merged vacuolar alterations. The drawback of this assumption is the presence of other features besides parenchyma in the image (*e.g.*, veins and artifacts).

Before creating the macro, we selected a subset of images with a broad range of characteristics (*e.g.*, number and size of vacuoles, staining properties, etc.). We then used these images to test a series of steps that would select all of the vacuoles in an image with the least amount of subjectivity (*i.e.*, altering of the threshold limits). During the course of this testing, the color deconvolution plugin (Landini, 2015) was found to give more precise delineation of the borders of vacuoles by using the basophilic image. In addition, the H&E 2 pre-defined vectors were found to work better for our images than the H&E vectors, likely because of the staining properties of our sections. Next, we used the ImageJ macro recorder. This produced a code that we adjusted to select the correct images for batch processing.

Before the batch processing was begun, we set scale globally as all images were taken with the same objective (20X). Then the macro was started. Briefly, the first image was retrieved and the color deconvolution plugin was run. This plugin separates co-stains into separate images, leaving a blank third image if only two stains were used; the unneeded images were closed. The remaining single image was thresholded and inverted. Simply, this made the white vacuoles black and the remaining tissue was converted to background white. The thresholded image was then converted to a mask and measured for area. This series of steps was completed for each image in the folder and output into a single Microsoft Excel file. All images (699) were analyzed in approximately 90 minutes on a standard laptop computer.

After the image processing was complete, the computed area values were averaged by section and then by individual. These averages were then compared to the semi-quantitative severity scores. The values were found to match in 44 out of 80 individuals (55%). From this, we conclude that this method works but needs additional refinement before it can be used independently of any visual characterization. Future work on the method will test Watershedding. Watershedding can separate merged vacuoles and

therefore allow us to define both size and circularity more narrowly. This should allow us to remove the influence of veins and artifacts while still allowing us to process heterogenic images. Additional routes of inquiry will be the efficacy of plugins used in other disciplines including ColonyArea (Guzmán *et al.*, 2014), IJBlob (Wagner and Lipinski, 2013), and Colony Blob Count Tool (Baecker, 2012), among others. The ultimate goal is to create a macro that can be used on any liver image to rapidly define and measure vacuolation.

ImageJ Java macro for quantifying liver vacuolation:

```
// This macro extracts and measures vacuolation in H&E stained sections
//Batch processes all of the files in the folder it is saved in, as such no getDirectory command is included at the beginning
//created by Amanda Riley and Melissa Chernick

title=getTitle();
run("Colour Deconvolution", "vectors=[H&E 2] hide");
selectImage(title+"-(Colour_3)");
close();
selectImage(title+"-(Colour_2)");
close();
selectImage(title+"-(Colour_1)");
setAutoThreshold("Default dark");
setOption("BlackBackground", false);
run("Convert to Mask");
run("Analyze Particles...", "size=0-Infinity circularity=0.00-1.00 show=Nothing summarize");
close(title+"-(Colour_1)");
close(title);
```

References

Baecker, V.(2012). Colony Blob Count Tool. Montpellier RIO Imaging, http://dev.mri.cnrs.fr/projects/imagej-macros/wiki/Colony_Blob_Count_Tool.

Collins, T.J. (2007). ImageJ for microscopy. *Biotechniques,* **43,** 25-30.

Guzmán, C., Bagga, M., Kaur, A., Westermarck, J. and Abankwa, D. (2014). ColonyArea: An ImageJ plugin to automatically quantify colony formation in clonogenic assays. *PLoS ONE,* **9,** e92444.

Homeyer, A., Schenk, A., Arlt, J., Dahmen, U., Dirsch, O. and Hahn, H.K. (2015). Fast and accurate identification of fat droplets in histological images. *Computer Methods and Programs in Biomedicine,* **121,** 59-65.

Landini, G.(2015). Color Deconvolution plugin In *NIH ImageJ 1.48* Web Site: http://www.mecourse.com/landinig/software/cdeconv/cdeconv.html.

Li, M., Song, J., Mirkov, S., Xiao, S.-Y., Hart, J. and Liu, W. (2011). Comparing morphometric, biochemical, and visual measurements of macrovesicular steatosis of liver. *Human Pathology,* **42,** 356-360.

Liquori, G.E., Calamita, G., Cascella, D., Mastrodonato, M., Portincasa, P. and Ferri, D. (2009). An innovative methodology for the automated morphometric and quantitative estimation of liver steatosis. *Histology and Histopathology,* **24,** 49-60.

Rasband, W.S.(2014). ImageJ 1.46. U. S. National Institutes of Health, Bethesda, Maryland, USA, Web Site: http://imagej.nih.gov/ij/.

Wagner, T. and Lipinski, H.-G. (2013). IJBlob: an ImageJ library for connected component analysis and shape analysis. *Journal of Open Research Software,* **1,** e6.

TABLE S1.—Individual PAH concentrations from collected Elizabeth River sediment and prepared ERSE.

SEDIMENT	ng/g	ERSE	ng/ml
Total PAH	**16,173,925**	***Total PAH***	**5044.7**
Phenanthrene	**4,213,796**	**Naphthalene**	**1617.2**
Fluoranthene	**2,812,499**	**Phenanthrene**	**597.1**
Pyrene	**2,130,274**	**Fluoranthene**	**422.6**
Acenaphthene	**1,874,111**	**Acenaphthene**	**404.7**
Anthracene	**1,153,186**	**Fluorene**	**321.2**
Fluorene	**939,343**	**Pyrene**	**288.0**
Dibenzofuran	553,889	Carbazole	246.0
Dibenzothiophene	248,711	Dibenzofuran	207.7
1,2-Benzanthracene	248,402	1-methylnaphthalene	161.5
2-methylphenanthrene	238,858	1,2-Benzanthracene	77.6
Chrysene	**230,792**	**Anthracene**	**73.1**
1-methylnaphthalene	203,218	Benzo(b)fluoranthene	66.1
2,6-dimethylnaphthalene	183,937	Dibenzothiophene	63.4
Naphthalene	**178,224**	**Chrysene**	**62.0**
Benzo(a)pyrene	**166,725**	Benzo(b)fluoranthene	47.9
1-methylphenanthrene	126,399	1,2-benzofluorene	46.5
Benzo(b)fluoranthene	120,589	2,6-dimethylnaphthalene	44.7
Benzo(e)pyrene	93,711	**Benzo(a)pyrene**	**44.3**
Benzo(k)fluoranthene	**82,365**	Retene	43.8
1,2-benzofluorene	80,482	2-methylphenanthrene	39.8
3,4-benzofluorene	64,978	Benzo(e)pyrene	31.2
Benzo(g,h,i)perylene	**56,470**	**Benzo(k)fluoranthene**	**26.6**
Perylene	48,221	1-methylphenanthrene	20.5
Benzo(c)phenanthrene	43,019	**Acenaphthylene**	**17.0**
Indeno(1,2,3-c,d)pyrene	**30,425**	**Benzo(g,h,i)perylene**	**14.7**
Benzo(a)fluoranthene	**20,225**	Picene	14.2
Acenaphthylene	**15,841**	3,4-benzofluorene	9.0
Retene	1,721	Perylene	8.8
Benzo(b)chrysene	1,163	**Benzo(a)fluoranthene**	**6.9**
Dibenzo(a,h)anthracene	**243**	Dibenzo(a,l)pyrene	6.2
Dibenzo(a,j)anthracene	187	**Indeno(1,2,3-c,d)pyrene**	**3.6**
Picene	149	Benzo(b)chrysene	3.5
Carbazole	46	Dibenzo(a,j)anthracene	2.8
Dibenzo(a,l)pyrene	36	**Dibenzo(a,h)anthracene**	**2.8**
		Benzo(c)phenanthrene	2.4

Bold compounds are included in the Environmental Protection Agency's priority list of 16 proven carcinogenic PAHs.

TABLE S2.—Severity index for semi-quantitative assessment of degree of vacuolation.

0 : Normal liver parenchyma; percent area ≤ 40%.
1 : Minimal, heterogeneous vacuole accumulation; percent area 41-50%.
2 : Mild, dispersive vacuole accumulation; percent area, 51-60%.
3 : Moderate accumulation of vacuoles associated with more than one hepatocyte; percent area 61-70%.
4 : Severe accumulation of vacuoles throughout the majority of the parenchyma with individual features as in 3 above; percent area, ≥71%.

TABLE S3.— Numbers of males and females based on gonadal tissue analysis and the square root transformed means of total alterations and basophilic foci. Female fish had significantly more total alterations (p=0.044) and basophilic foci (p=0.036) (*e.g.*, Figure 6B) than did males.

		Female (N=37)	**Male (N=37)**
Atlantic Wood	Control	6	7
	0.1%	5	5
	1.0%	8	6
King's Creek	Control	8	8
	0.1%	4	6
	1.0%	6	5
Mean Total Alterations		1.53[a]	1.20[b]
Mean Basophilic Foci		1.29[a]	0.93[b]

Different letters indicate statistical differences for mean alterations within row. One-way ANOVA with post-hoc Tukey test ($p \leq 0.05$).

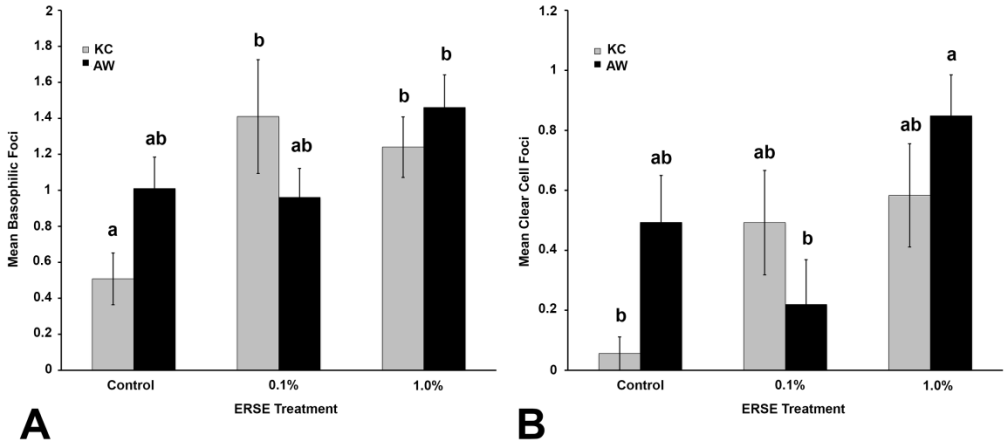

SUPPLEMENTARY FIGURE 1 (S1).— Histograms representing alterations in basophilic foci (*A*) and clear cell foci (*B*) in King's Creek (*gray bars*) and Atlantic Wood (*black bars*) populations across all ERSE treatment groups. Bars are means of transformed data with error bars representing standard error of the mean. Different letters above histogram bars indicate statistical differences. Nested ANOVA with post-hoc Tukey test ($p \leq 0.05$).

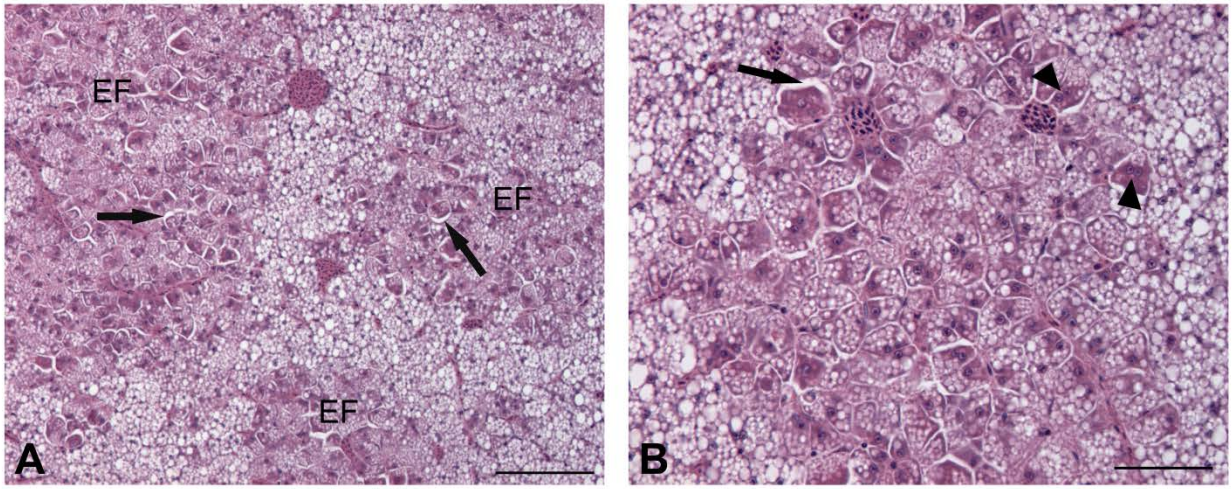

SUPPLEMENTARY FIGURE 2 (S2).— Eosinophilic foci (*EF) in an AW control fish. A, eosinophilic foci (EF). Scale bar 10 µm, 20X, H&E. B, eosinophilic focus showing enlarged and bi-nucleated hepatocytes (arrowheads). Scale bar 5 µm, 40X, H&E. Arrows, inter-hepatocytic spaces which may indicate loss of contact inhibition enabling cells to divide.*